International Journal of Nanomedicine

Dovepress
open access to scientific and medical research

Open Access Full Text Article

ORIGINAL RESEARCH

Energy-dependent endocytosis is responsible for drug transcorneal penetration following the instillation of ophthalmic formulations containing indomethacin nanoparticles

This article was published in the following Dove Medical Press journal:
International Journal of Nanomedicine

Noriaki Nagai[1]
Fumihiko Ogata[1]
Hiroko Otake[1]
Yosuke Nakazawa[2]
Naohito Kawasaki[1]

[1]Faculty of Pharmacy, Kindai University, Higashi-Osaka 577-8502, Japan; [2]Faculty of Pharmacy, Keio University, Minato-ku, Tokyo 105-8512, Japan

Purpose: We previously found that ophthalmic formulations containing nanoparticles prepared by a bead mill method lead to an increase in bioavailability in comparison with traditional formulations (solution type). However, the transcorneal penetration pathway for ophthalmic formulations has not been explained yet. In this study, we investigated the mechanism of transcorneal penetration in the application of ophthalmic formulations containing indomethacin nanoparticles (IMC-NPs).

Materials and methods: IMC-NPs was prepared by the bead mill method. For the analysis of energy-dependent endocytosis, corneal epithelial (HCE-T) cell monolayers and removed rabbit cornea were thermoregulated at 4°C, where energy-dependent endocytosis is inhibited. In addition, for the analysis of different endocytosis pathways using pharmacological inhibitors, inhibitors of caveolae-mediated endocytosis (54 μM nystatin), clathrin-mediated endocytosis (40 μM dynasore), macropinocytosis (2 μM rottlerin) or phagocytosis (10 μM cytochalasin D) were used.

Results: The ophthalmic formulations containing 35–200 nm sized indomethacin nanoparticles were prepared by treatment with a bead mill, and no aggregation or degradation of indomethacin was observed in IMC-NPs. The transcorneal penetration of indomethacin was significantly decreased by the combination of nystatin, dynasore and rottlerin, and the decreased penetration levels were similar to those at 4°C in HCE-T cell monolayers and rabbit cornea. In the in vivo experiments using rabbits, dynasore and rottlerin tended to decrease the transcorneal penetration of indomethacin (area under the drug concentration – time curve in the aqueous humor [AUC_{AH}]), and the AUC_{AH} in the nystatin-treated rabbit was significantly lower than that in non-treatment group. In addition, the AUC_{AH} in rabbit corneas undergoing multi-treatment was obviously lower than that in rabbit corneas treated with each individual endocytosis inhibitor.

Conclusion: We found that three energy-dependent endocytosis pathways (clathrin-dependent endocytosis, caveolae-dependent endocytosis and macropinocytosis) are related to the transcorneal penetration of indomethacin nanoparticles. In particular, the caveolae-dependent endocytosis is strongly involved.

Keywords: drug delivery system, bead mill, caveolae-dependent endocytosis, clathrin-dependent endocytosis, macropinocytosis

Plain language summary

We previously found that the corneal penetration of ophthalmic formulations containing nanoparticles is higher in comparison with traditional formulations (solution type), although the transcorneal penetration pathway for the ophthalmic formulations has not yet been explained. In this study, we elucidate the mechanism of transcorneal penetration in the application of ophthalmic formulations containing indomethacin nanoparticles (IMC-NPs). Briefly, indomethacin nanoparticles are taken up

Correspondence: Noriaki Nagai
Faculty of Pharmacy, Kindai University, 3-4-1 Kowakae, Higashi-Osaka 577-8502, Japan
Tel +81 6 4307 3640
Fax +81 6 6730 1394
Email nagai_n@phar.kindai.ac.jp

submit your manuscript | www.dovepress.com
Dovepress
http://dx.doi.org/10.2147/IJN.S196681

into the corneal epithelium by energy-dependent endocytosis pathways (clathrin-dependent endocytosis, caveolae-dependent endocytosis and macropinocytosis), especially caveolae-dependent endocytosis, and cross to the corneal stromal side. From there, the indomethacin nanoparticles dissolve in the cornea, and are released into the aqueous humor in a soluble form. Our studies are the first to characterize the relationship of drug solid nanoparticles and drug delivery by energy-dependent endocytosis in the cornea, and the results provide significant information that can be used to design further studies aimed at developing ophthalmic nanomedicines.

Introduction

Indomethacin, [1-(4-chlorobenzoyl)–5-methoxy-2-methylindol-3-yl] acetic acid, a topical non-steroidal anti-inflammatory drug (NSAID), is used in the treatment of ocular inflammatory disorders such as anterior segment inflammation, uveitis, conjunctivitis, macular edema, cystoid and post-operative pain following cataract surgery.[1–3] Topically applied indomethacin blocks the cyclooxygenase enzymes and inhibits prostaglandin synthesis, thereby controlling the associated inflammation.[4,5] Topical administration (eg, eye drops) is the most attractive method of administration owing to its ease of application, more limited side effects than systemic administration, and high patient comfort and compliance, and is the major delivery route used for optimal drug absorption in therapy for anterior segment diseases such as inflammation.[6] However, eye drops (traditional formulations) are often eliminated rapidly from the pre-corneal area by tear turnover, tear dilution and lacrimation (various physiological mechanisms), and in addition tissue barriers (conjunctiva, cornea, sclera and lens) are present.[7,8] All these barriers reduce the bioavailability (BA) in the cornea to $<5\%$.[9] Therefore, approaches that improve the pre-corneal residence time and transcorneal permeability characteristics are expected.

It is considered that improvements in the precorneal residence times and corneal permeability of drugs can increase their BA. Nanotechnology is a general term used for technologies that use the properties of nanoscale substances to develop new functions for these substances and improve their properties. Among ophthalmic drugs, delivery systems (DDS) for which formulation strategies have been tested include the application of solutions, suspensions, emulsions, liposomes, surfactant-based systems, nanomicelles, microspheres, nanospheres, solid nanoparticles, polymeric nanoparticles, implants and gelling systems.[10–12] We also designed solid nanoparticles created by a breakdown mill (bead mill method), and reported on the properties of low corneal stimulation and high transcorneal penetration of formulations containing solid nanoparticles in comparison with traditional formulations (liquid formulations and ophthalmic suspensions).[13–17] It is expected that solid nanoparticles may increase absorption and BA, and provide a novel strategy for transcorneal DDS. However, the mechanism of nanoparticle transport through the cornea is not fully understood.

Nanoparticles do not enter cells simply via diffusion. Recently, Majumder et al[18] designed a multicompartment hydrogel, and reported that the endocytosis pathway is related to the penetration of drug-loaded nanoparticles/hydrogels into the cell and nucleus, and the relationship between endocytosis and nanoparticle-based drug delivery has been revealed by many researchers.[19–23] Endocytosis is generally classified as phagocytosis (originally discovered in macrophages) and pinocytosis [clathrin-dependent endocytosis (CME), caveolae-dependent endocytosis (CavME), and macropinocytosis (MP)].[24,25] The sizes corresponding to CME, CavME and MP are <120 nm, <80 nm and 100 nm to 5 μm, respectively.[26] Endocytosis inhibitors are drugs that specifically block individual cellular uptake pathways,[27–30] while incubation at a cold temperature (4°C) inhibits all energy-dependent uptake, including endocytosis, in cells.[31] Experiments using inhibitors and cold conditions are useful for evaluating the mechanisms of nanoparticle-based drug delivery systems. In this study, we investigated the mechanism of transcorneal penetration in the application of ophthalmic formulations containing indomethacin nanoparticles (IMC-NPs) using endocytosis inhibitors and cold conditions.

Materials and methods

Animals

Adult Japanese albino rabbits weighing ~2.7 kg were purchased from Shimizu Laboratory Supplies Co., Ltd (Kyoto, Japan), and allowed free access to a CR-3 commercial diet (Clea Japan Inc., Tokyo, Japan) and water. The rabbits were housed under standard conditions (light 7:00–19:00/dark 19:00–7:00, 25°C). All experiments using rabbits were carried out in accordance with the Pharmacy Committee Guidelines for the Care and Use of Laboratory Animals in Kindai University, and approved on 1 April 2013 (project identification code KAPS-25-003). In addition, all procedures were in accordance with the Guiding Principles approved by the ARVO resolution on the use of animals in research.

Chemicals

Indomethacin powder (particle size, 5.01±0.59 μm), cytochalasin D, isoflurane, mannitol (D-mannitol) and propyl p-hydroxybenzoate were purchased from Wako Pure

Chemical Industries, Ltd (Osaka, Japan). 2-Hydroxypropyl-β-cyclodextrin (HPβCD) was obtained from Nihon Shokuhin Kako Co., Ltd (Tokyo, Japan), and nystatin and rat tail collagen type 1, was provided by Sigma-Aldrich Japan (Tokyo, Japan). Methylcellulose (MC, type SM-4) with an average viscosity of ~4 Pa·s at 20°C was obtained from Shin-Etsu Chemical Co., Ltd (Tokyo, Japan). Dynasore and rottlerin were purchased from Nacalai Tesque (Kyoto, Japan), and benzalkonium chloride (BAC) was provided by Kanto Chemical Co., Inc. (Tokyo, Japan). Dulbecco's Modified Eagle's Medium/Ham's F12, heat-inactivated fetal bovine serum, streptomycin and penicillin were obtained from Gibco (Thermo Fisher Scientific, Waltham, MA, USA). TetraColor One was purchased from Seikagaku Co. (Tokyo, Japan). All other chemicals used were of the highest purity commercially available.

Preparation of ophthalmic IMC-NPs

Indomethacin nanoparticles were prepared following our previous reports using zirconia beads (diameter: 0.1 mm) and Bead Smash 12 (a bead mill, Wakenyaku Co. Ltd, Kyoto, Japan).[15] Indomethacin powder (microparticles), BAC, mannitol and MC were mixed in HPβCD solution (IMC-MPs), and crushed with the Bead Smash 12 (IMC-NPs). The conditions for the bead mill were as follows: 5,500 rpm for 30 seconds 30 times at 4°C. The compositions of the IMC-MPs and IMC-NPs were as follows: 1.5% indomethacin, 0.001% BAC, 0.1% mannitol, 2% MC, 5% HPβCD. 1.5% IMC-NPs is equivalent to 41.9 mM indomethacin; the pH was 6.5. Liquid indomethacin (IMC-solution) was prepared by dissolving in 0.5% dimethyl sulfoxide (DMSO). The zeta potential was measured by a micro-electrophoresis zeta potential analyzer model 502 (Nihon Rufuto Co., Ltd, Tokyo, Japan).

Particle image and size of indomethacin

Particle images were obtained under an atomic force microscope (AFM) using SPM-9700 (Shimadzu Corp., Kyoto, Japan). The AFM image of IMC-NPs was created by combining a phase and height image. The particle size of indomethacin was measured by dynamic light scattering Nanosight LM10 (QuantumDesign Japan, Tokyo, Japan), a laser diffraction particle size analyzer SALD-7100 (Shimadzu Corp.); the number of indomethacin nanoparticles was also determined using the Nanosight LM10. The conditions for Nanosight LM10 were as follows: measurement time, 60 seconds; wavelength, 405 nm (blue); viscosity of the suspension, 1.27 mPa·s. The refractive index was set at 1.60–0.010i in the SALD-7100.

Measurement of indomethacin by HPLC

Indomethacin concentrations in the samples were measured by a LC-20AT system (HPLC, Shimadzu Corp.) with 1 μg/mL propyl p-hydroxybenzoate used as an internal standard. An Inertsil® ODS-3 column (2.1 × 50 mm, GL Science Co., Inc., Tokyo, Japan) was used at 35°C, and the wavelength for detection was 254 nm. The mobile phase consisted of acetonitrile/50 mM acetic acid (40/60, v/v) at a flow rate of 0.25 mL/min.

Dispersibility of IMC-NPs

The experiment was performed according to our previous report.[15] Three milliliter samples of IMC-NPs were incubated in 5 mL test tubes in the dark at 20°C for 14 days, and 50 μL samples of the solutions were withdrawn from 5 mm under the surface at the indicated time intervals (total height of liquid, 4 cm). The dispersibility of IMC-NPs was evaluated by measuring the concentration, particle size and nanoparticle number by the HPLC and NANOSIGHT LM10 methods described above.

Corneal penetration of indomethacin using corneal epithelial cell monolayers

The immortalized human cornea epithelial cell line (HCE-T) was developed by Araki-Sasaki et al,[32] and were purchased from Riken BioResource Research Center (Ibaraki, Japan). All experiments using HCE-T cells were carried out in accordance with the Pharmacy Committee Guidelines for the Safety Committee for Recombinant DNA Experiments in Kindai University, and approved on 1 April 2012 (project identification code KDPS-12-002). The HCE-T cells were cultured in Dulbecco's Modified Eagle's Medium/Ham's F12 containing 5% (v/v) heat-inactivated fetal bovine serum, 0.1 mg/mL streptomycin and 1,000 IU/mL penicillin. HCE-T cell monolayers were prepared according to our previous study.[33] Briefly, HCE-T cells (90,000 cells/cm^2) were seeded onto Transwell-Clear™ (Costar, Cambridge, MA, USA) coated with 71.5 μg/cm^2 rat tail collagen type 1, and grown for 7 days. After that, the HCE-T cells were exposed to an air–liquid interface for 14 days. In this study, transepithelial electrical resistance (TER) was measured using an epithelial Volt-Ohm meter (Millicell-ERS, EMD Millipore, Billerica, MA, USA), and the groups with TER values >300 Ω·cm^2 were used for permeation studies. The accumulation and permeation of indomethacin were studied by adding 1.5 mL Hank's balanced salt solution (pH 7.4) containing 25 mM HEPES (HBSS/HEPES solution) to the basolateral side (reservoir chamber) of the monolayer,

and 0.5 mL vehicle or ophthalmic formulations containing 0.15% indomethacin to the apical side (donor chamber). The concentration (0.15%) was determined taking dilution by the lacrimal fluid into account (10-fold dilution). The TER values were measured for 0–60 min, and the penetration experiments were performed for 30 minutes by removing 10 µL of sample solution from the reservoir chamber. In addition, cells were collected 30 minutes after treatment. The indomethacin concentration, particle size and nanoparticle number were obtained by the HPLC methods and Nanosight LM10 as described above.

Transcorneal penetration of indomethacin formulation using isolated rabbit cornea

The in vitro transcorneal penetration of 1.5% IMC-NPs was examined using the method described in our previous report.[13] Rabbits were killed by injecting a lethal dose of pentobarbital into the marginal ear vein, and the corneas were removed. The individual corneas were set on a methacrylate cell (transcorneal cell) designed for transcorneal penetration experiments. The donor chamber (exterior surface of the cornea side) was filled with indomethacin formulations, and the other side of the chamber (reservoir chamber) was filled with HEPES buffer (10 mM, pH 7.4) containing NaCl (136.2 mM), KCl (5.3 mM), K_2HPO_4 (1 mM), $CaCl_2$ (1.7 mM) and glucose (5.5 mM). The experiments were performed at 4°C or 37°C for 6 hours, and the indomethacin concentrations were determined by the HPLC method described above. The obtained data were evaluated by the following Equations 1–3:

$$J_c = \frac{K_m \cdot D \cdot C_{IMC}}{\delta} = K_p \cdot C_{IMC} \quad (1)$$

$$\tau = \frac{\delta^2}{6D} \quad (2)$$

$$Q_t = J_c \cdot A \cdot (t - \tau) \quad (3)$$

where J_c, K_p, K_m, D, C_{IMC}, τ, δ, Q_t and A are the indomethacin penetration rate, penetration coefficient through the cornea, cornea/preparation partition coefficient, diffusion constant within the cornea, indomethacin content in the ophthalmic formulation, lag time, thickness of the cornea, total amount of indomethacin appearing in the reservoir solution at time t and effective area of the cornea, respectively. The area under the drug concentration–time curve in the reservoir chamber ($AUC_{penetration}$) was determined according to the trapezoidal rule up to the last indomethacin concentration measurement point (6 hours).

In vivo transcorneal penetration of IMC-NPs

The in vivo transcorneal penetration of IMC-NPs was determined following our previous reports.[13,15] Rabbits were anesthetized with isoflurane, and a topical anesthetic (0.4% Benoxil) was instilled into each eye 3 minutes before sampling of the aqueous humor. Samples of aqueous humor (5 µL each) were collected, and the indomethacin concentrations in the aqueous humor were determined by HPLC as described above. The area under the drug concentration–time curve in the aqueous humor (AUC_{AH}) was determined according to the trapezoidal rule up to the last indomethacin concentration measurement point (90 minutes).

Inhibitor of energy-dependent endocytosis

For the analysis of energy-dependent endocytosis, HCE-T cell monolayers and removed rabbit corneas were thermoregulated at 4°C where energy-dependent endocytosis is inhibited[31] or at 37°C (normal conditions). For the analysis of different endocytosis pathways (CavME, CME, MP and phagocytosis), pharmacological inhibitors specific to each were used. CavME was inhibited by 54 µM nystatin, which acts by binding to plasma membrane cholesterol.[34] CME was inhibited by 40 µM dynasore, a specific and highly effective blocker of dynamin, one of the key proteins in the endocytosis machinery of synaptic vesicles.[35] MP was inhibited by 2 µM rottlerin, a selective inhibitor of fluid-phase endocytosis.[36] Finally, phagocytosis was inhibited by 10 µM cytochalasin D, which blocks actin polymerization and disassembly of the actin cytoskeleton.[34] In experiments using HCE-T cell monolayers, the specific inhibitors were applied for 5 minutes, 1 hour prior to treatment with IMC-NPs. In experiments using removed rabbit corneas, the transcorneal cell (reservoir chamber) was filled with HEPES buffer with or without endocytosis inhibitor. In the in vivo studies of transcorneal penetration, 30 µL of endocytosis inhibitor was instilled 3 times prior to treatment with IMC-NPs. All endocytosis inhibitors were dissolved in 0.5% DMSO.

Statistical analysis

The data from the laser diffraction particle size analyzer (SALD-7100) are expressed as mean ± SD; other data are expressed as mean ± standard error (SE) of the mean. The sample numbers (n) are shown in the figure legends. Student's

t-test was used for two group comparisons, and one-way ANOVA followed by Dunnett's multiple comparison was used for multiple group comparisons. A minimum *P*-value of 0.05 was chosen as the significance level ($P<0.05$).

Results

Evaluation of IMC-NPs stability

Size and shape are the most important factors in the transport pathways for nanoparticles. Therefore, we investigated the particle size frequency and shape of indomethacin in IMC-NPs by Nanosight LM10 and AFM imaging, respectively. Figure 1 shows the particle size frequencies, image and solubility of indomethacin in the IMC-NPs. The mean particle size in the microparticles was 5.01±0.59 μm, and the particle size was decreased by the bead mill treatment to 83±121 nm as determined using a laser diffraction particle size analyzer. We also measured the particle size by a dynamic light scattering method and atomic force microscope, which

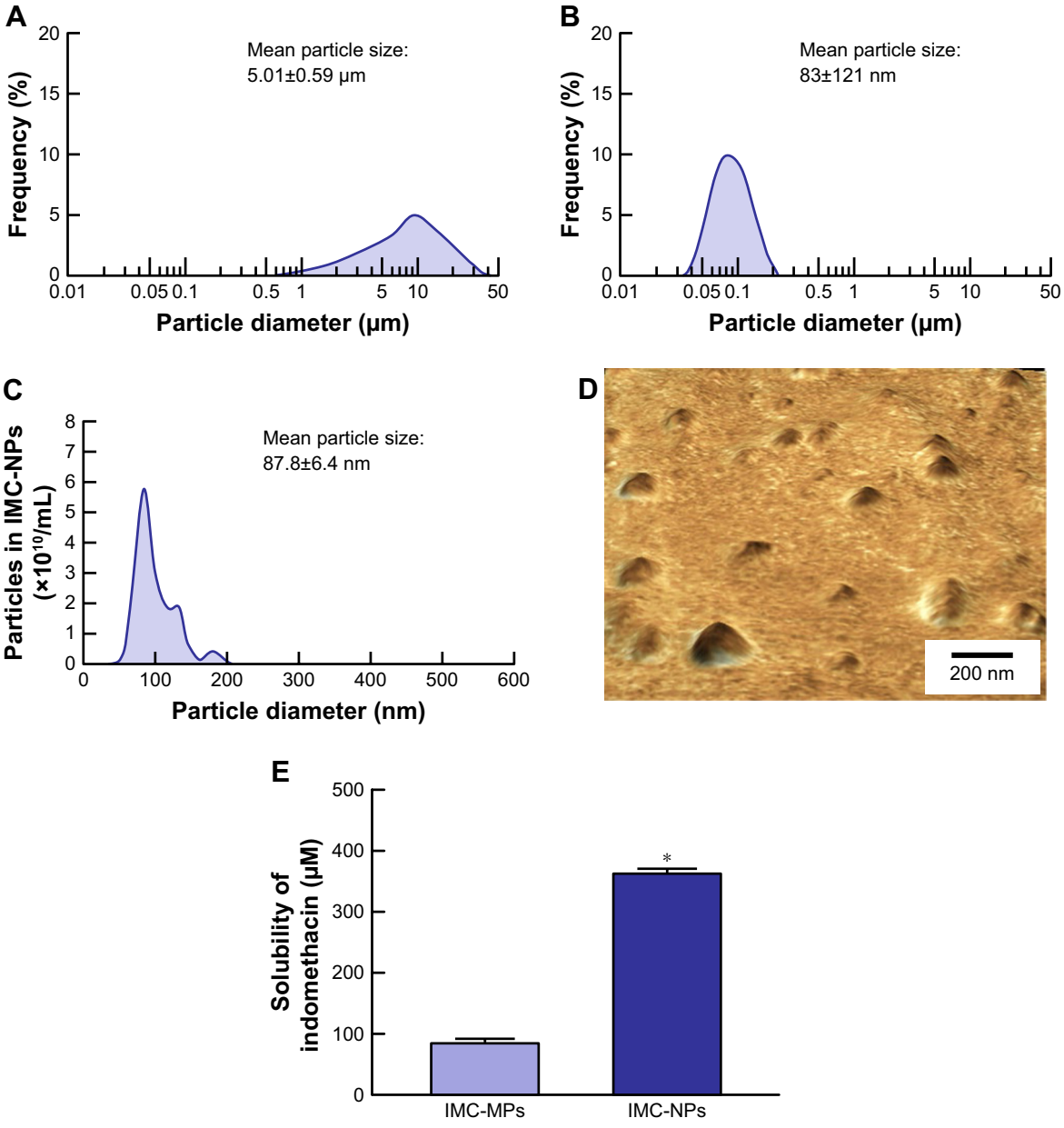

Figure 1 Particle size frequencies and solubility of indomethacin in IMC-NPs.

Notes: Particle size frequencies of indomethacin in IMC-MPs (**A**) and IMC-NPs (**B**) as determined by a laser diffraction particle size analyzer. (**C**) Particle size frequencies of indomethacin in IMC-NPs by the dynamic light scattering method. (**D**) AFM image of indomethacin in IMC-NPs by the SPM-9700. (**E**) Solubility of indomethacin in IMC-NPs. n=8. *$P<0.05$ vs IMC-MPs. The ophthalmic formulation containing 35–200 nm sized indomethacin nanoparticles was prepared by treatment with a bead mill. The drug solubility in IMC-MPs and IMC-NPs was higher than that in IMC-MPs at 84.5 μM and 363.2 μM, respectively.

Abbreviations: IMC-MPs, ophthalmic formulation containing indomethacin microparticles; IMC-NPs, ophthalmic formulation containing indomethacin nanoparticles.

showed a mean particle size of 87.8±6.4 nm and 79.1±4.7 nm, respectively. It was already known that solubility is enhanced for nanoparticles. The solubility of indomethacin in IMC-NPs (363.2 μM, 0.013%) was higher than that in IMC-MPs (84.5 μM, 0.003%); however, this level is still small with a ratio of 0.0086% for IMC-NPs (1.5%). The zeta potential of IMC-NPs was −12.1 mV. Figure 2 shows the changes in particle size, number, form and concentration 14 days after the production of IMC-NPs. The particle size was 168.3±4.1 nm, and the number of indomethacin nanoparticles in IMC-NPs was $2.76\pm0.18\times10^{12}$ particles/mL. The particle size and number 14 days after preparation were similar to those immediately after bead mill treatment ($2.61\pm0.11\times10^{12}$ particles/mL). In addition, no changes in dispersibility, form and concentration were observed 14 days after bead mill treatment. Moreover, the dissolved indomethacin levels in the IMC-NPs were not changed 14 days after preparation (368±6.9 μm). These data show that it is possible to prepare

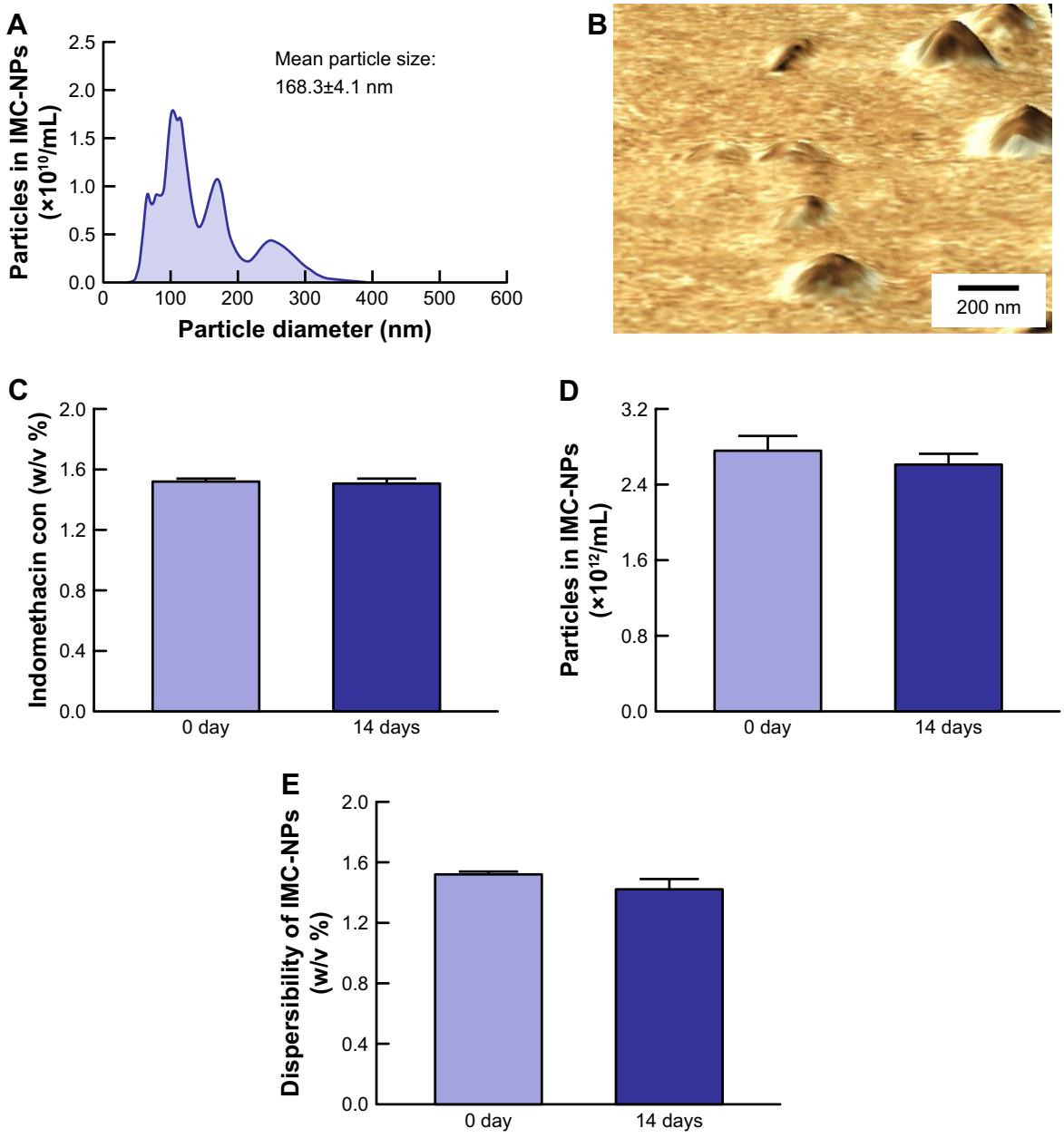

Figure 2 Stability of IMC-NPs 14 days after bead mill treatment.
Notes: Particle size frequencies (**A**) and AFM image (**B**) of indomethacin in IMC-NPs by the dynamic light scattering method and SPM-9700, respectively. Changes in concentration (**C**), particle number (**D**) and dispersibility (**E**) of indomethacin in IMC-NPs. n=8. No aggregation or degradation of indomethacin was observed in IMC-NPs, and the size of the indomethacin particles in IMC-NPs remained in the nano order for 14 days.
Abbreviations: IMC-NPs, ophthalmic formulation containing indomethacin nanoparticles; con, concentration.

ophthalmic formulations containing 1.5% indomethacin nanoparticles by the bead mill method using BAC, mannitol, MC and HPβCD.

Determination of the energy-dependent endocytosis pathway for indomethacin nanoparticles using HCE-T cell monolayers

Since endocytosis is the major route by which nanomedicines are transported across membranes,[24,25,37] we investigated the relationships between endocytosis and indomethacin nanoparticles in corneal penetration. Figure 3 shows the transepithelial penetration profiles for indomethacin nanoparticles under cold conditions of inhibited energy-dependent endocytosis (4°C) and normal conditions (37°C) in HCE-T cell monolayers. The TER value remained >300 Ω·cm^2 in HCE-T cell monolayers incubated at cold or normal temperatures. In HCE-T cell monolayers treated with IMC-solution and IMC-MPs, the accumulation and penetration showed no difference between normal and cold conditions.

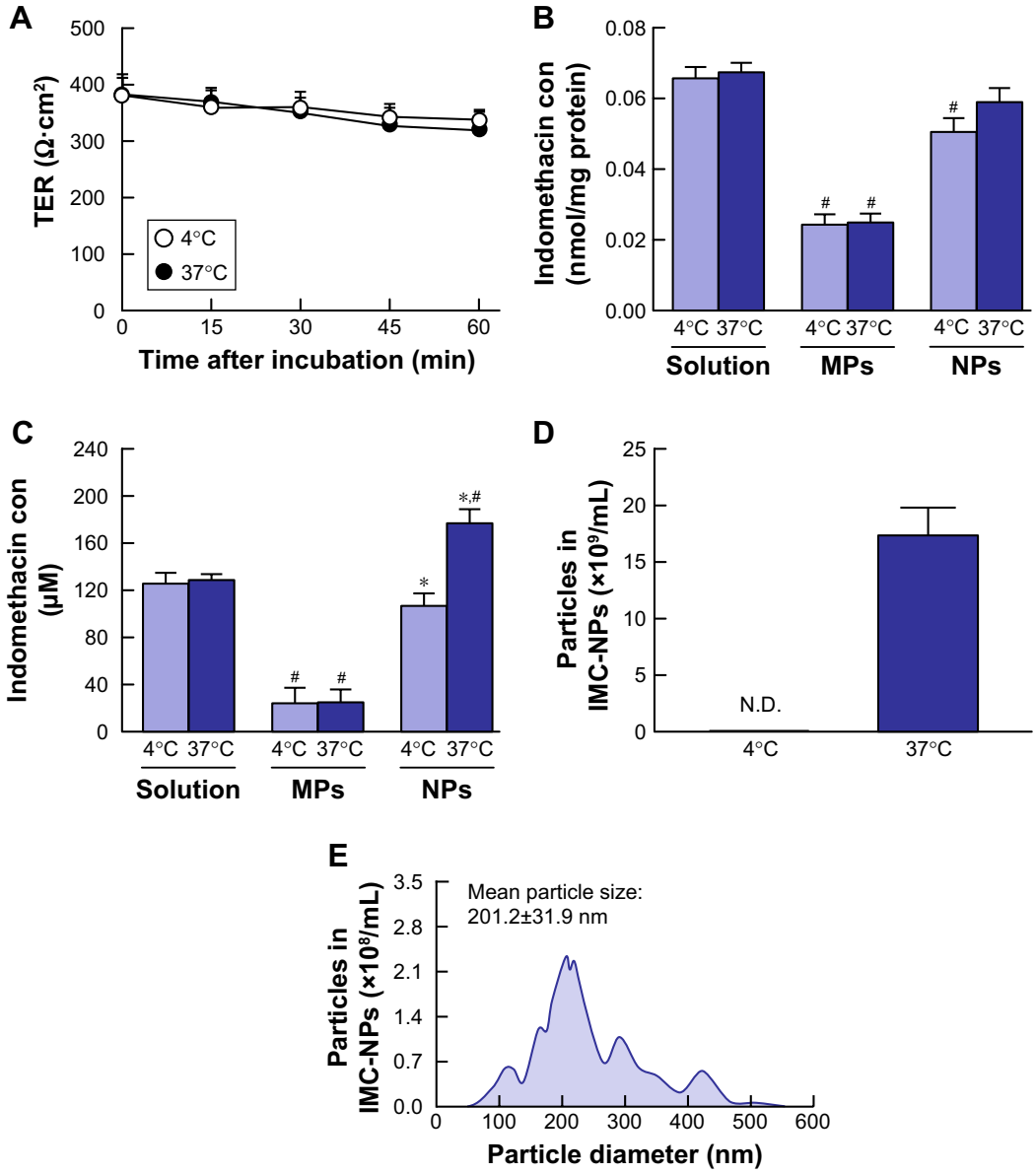

Figure 3 Transepithelial penetration of indomethacin in IMC-NPs at 4°C and 37°C using HCE-T cell monolayers.

Notes: (**A**) Changes of TER in HCE-T cell monolayers treated with IMC-NPs 4°C and 37°C. Accumulation (**B**) and penetration (**C**) of indomethacin in HCE-T cells treated with IMC-solution, IMC-MPs and IMC-NPs, at 4°C and 37°C. Number (**D**) and size frequencies (**E**) of indomethacin nanoparticles in the basolateral side at 4°C conditions. n=6. *$P<0.05$ vs 37°C conditions for each category. #$P<0.05$ vs IMC solution at 37°C conditions. The accumulation of indomethacin tended to be less at 4°C, and transepithelial penetration was significantly prevented at 4°C.

Abbreviations: IMC-MPs, ophthalmic formulation containing indomethacin microparticles; IMC-NPs, ophthalmic formulation containing indomethacin nanoparticles; con, concentration; TER, transepithelial electrical resistance.

In contrast with the results of IMC-solution and IMC-MPs, the accumulation in the HCE-T cell monolayers incubated at cold temperature tended to be lower than in HCE-T cell monolayers incubated at normal temperature in the IMC-NPs. Moreover, the penetration of indomethacin in IMC-NPs was significantly prevented in HCE-T cell monolayers incubated at cold temperature. Although nanoparticles were observed on the basolateral side at 37°C, no nanoparticles were detectable at 4°C. Figure 4 shows changes in the accumulation and penetration of indomethacin from the IMC-NPs into HCE-T cell monolayers co-treated with indomethacin formulation and endocytosis inhibitors. The TER values in HCE-T cell monolayers treated with endocytosis inhibitors were decreased to less than the 300 $\Omega \cdot cm^2$ by treatment for 45 minutes and 60 minutes. In addition, we measured the HCE-T cell viability 30 minutes after treatment with endocytic inhibitors using the TetraColor One. The cell viability following treatment with nystatin, dynasore, rottlerin or cytochalasin D individually and with multi-treatment (nystatin, dynasore and rottlerin) were 96.3%±1.5%, 96.8%±1.3%, 95.9%±1.9%, 98.3%±2.1% and 93.4%±2.6%, respectively (ratio for treatment/non-treatment, mean ± SE, n=10). Therefore, the accumulation and penetration in HCE-T cell monolayers treated with indomethacin formulation was measured 30 minutes after the addition of endocytosis inhibitors. Treatment with dynasore or rottlerin tended to prevent the penetration of indomethacin in IMC-NPs, while the penetration of indomethacin in IMC-NPs was significantly prevented by treatment with nystatin. Indomethacin nanoparticles were detected on the basolateral side, and their numbers were also lower in groups treated with nystatin, dynasore or rottlerin. In addition, the accumulation, penetration and particle number of indomethacin were all significantly lower in HCE-T cells treated simultaneously with nystatin, dynasore and rottlerin, with accumulation and penetration values 86% and 70% of those of vehicle-treated cells.

Effect of energy-dependent endocytosis on the transcorneal penetration of indomethacin nanoparticles using rabbit corneas

Figure 5 shows the changes in the accumulation and penetration of indomethacin particles from the IMC-NPs into rabbit corneas treated with cold temperature and endocytosis inhibitors. Table 1 summarizes the pharmacokinetic parameters estimated from the data for the in vitro transcorneal penetration shown in Figure 5. At 4°C, corneal penetration was decreased, with an $AUC_{penetration}$ 22.7% of that under normal conditions. In the experiment using endocytosis inhibitors, the transcorneal penetration was similar between the vehicle and cytochalasin D-treated groups. However, treatment with nystatin, rottlerin or dynasore all significantly prevented the corneal penetration of indomethacin in IMC-NPs. In addition, the $AUC_{penetration}$ in corneas treated with nystatin, dynasore and rottlerin together was also significantly lower than in vehicle-treated corneas with levels similar to that at 4°C (inhibited energy-dependent endocytosis). Moreover, no indomethacin nanoparticles were detected in the reservoir chamber after the addition of the IMC-NPs under either 4°C or 37°C conditions. Figure 6 shows the changes in the amount of indomethacin in the aqueous humor after the instillation of IMC-NPs in rabbits pre-treated with endocytosis inhibitors. The AUC_{AH} in rabbits treated with cytochalasin D was similar to the vehicle groups. On the other hand, the corneal penetration (AUC_{AH}) was significantly decreased by treatment with nystatin, dynasore or rottlerin, with the AUC_{AH} in nystatin-treated corneas only 34.0% that of the control. In addition, the AUC_{AH} in the multi-treatment group (nystatin, dynasore and rottlerin) was 17.5%, obviously lower than in the vehicle group.

Discussion

Although topically applied indomethacin is commonly used for the management and prevention of ocular inflammation and intraocular irritation after cataract extraction, its clinical use is limited by its low BA and corneal damage.[38] On the other hand, we previously found that nanoparticle formulations prepared by a bead mill method lead to an increase in BA, and the corneal toxicity of ophthalmic formulations containing nanoparticles is lower than that of traditional formulations (solution type).[13–17] In addition, we previously produced an ophthalmic formulation containing 0.5% indomethacin nanoparticles that showed high transcorneal penetration.[15] However, it is important to design ophthalmic formulations containing a higher content of drug nanoparticles in order to enhance the corneal penetration and duration. In addition, the transcorneal penetration pathway for ophthalmic formulations containing nanoparticles has not yet been explained. In this study, we designed an ophthalmic formulation containing 1.5% indomethacin solid nanoparticles (high content type), and found that three energy-dependent endocytosis pathways (CavME, CME and MP) are related to the transcorneal penetration of indomethacin nanoparticles; in particular, the CavME pathway is strongly involved.

In the preparation of IMC-NPs, additives were selected as described in our previous reports, and the bead mill method was used. BAC (0.001%–0.02%), commonly used in the

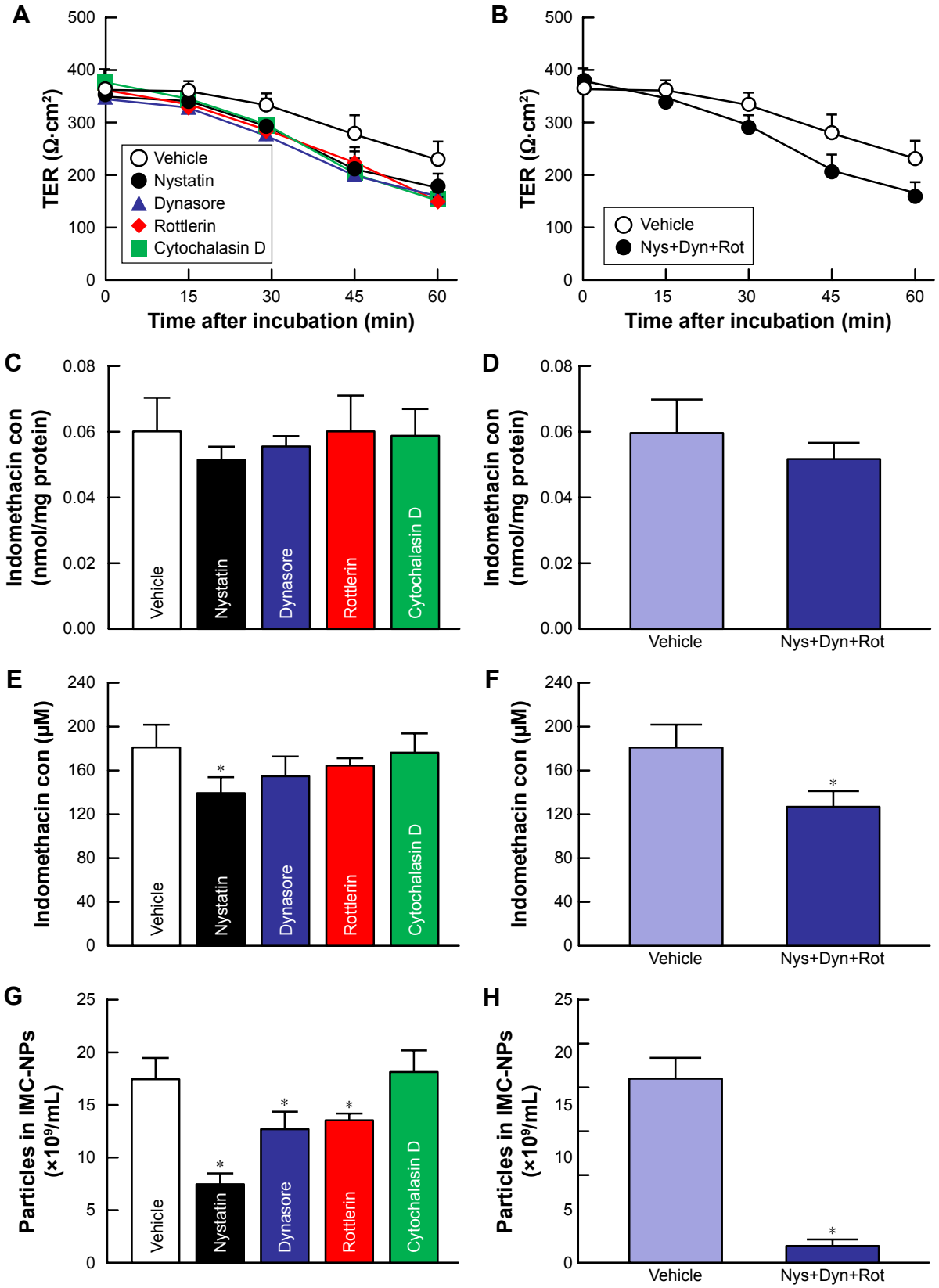

Figure 4 Effect of endocytosis pathways on transepithelial penetration of IMC-NPs in HCE-T cell monolayers.

Notes: Effects of endocytosis inhibitors on the TER (**A**), accumulation (**C**) and penetration (**E**) of indomethacin in HCE-T cell monolayers treated with IMC-NPs. Changes in TER (**B**), accumulation (**D**) and penetration (**F**) of indomethacin in HCE-T cell monolayers treated with IMC-NPs by multi-treatment with nystatin, dynasore and rottlerin (Nys+Dyn+Rot). (**G** and **H**) Effect of endocytosis inhibitors on the number of indomethacin nanoparticles in the basolateral side. n=5–8. *$P<0.05$ vs vehicle for each category. The penetration of indomethacin was significantly decreased by the combination of nystatin, dynasore and rottlerin.

Abbreviations: IMC-NPs, ophthalmic formulation containing indomethacin nanoparticles; con, concentration.

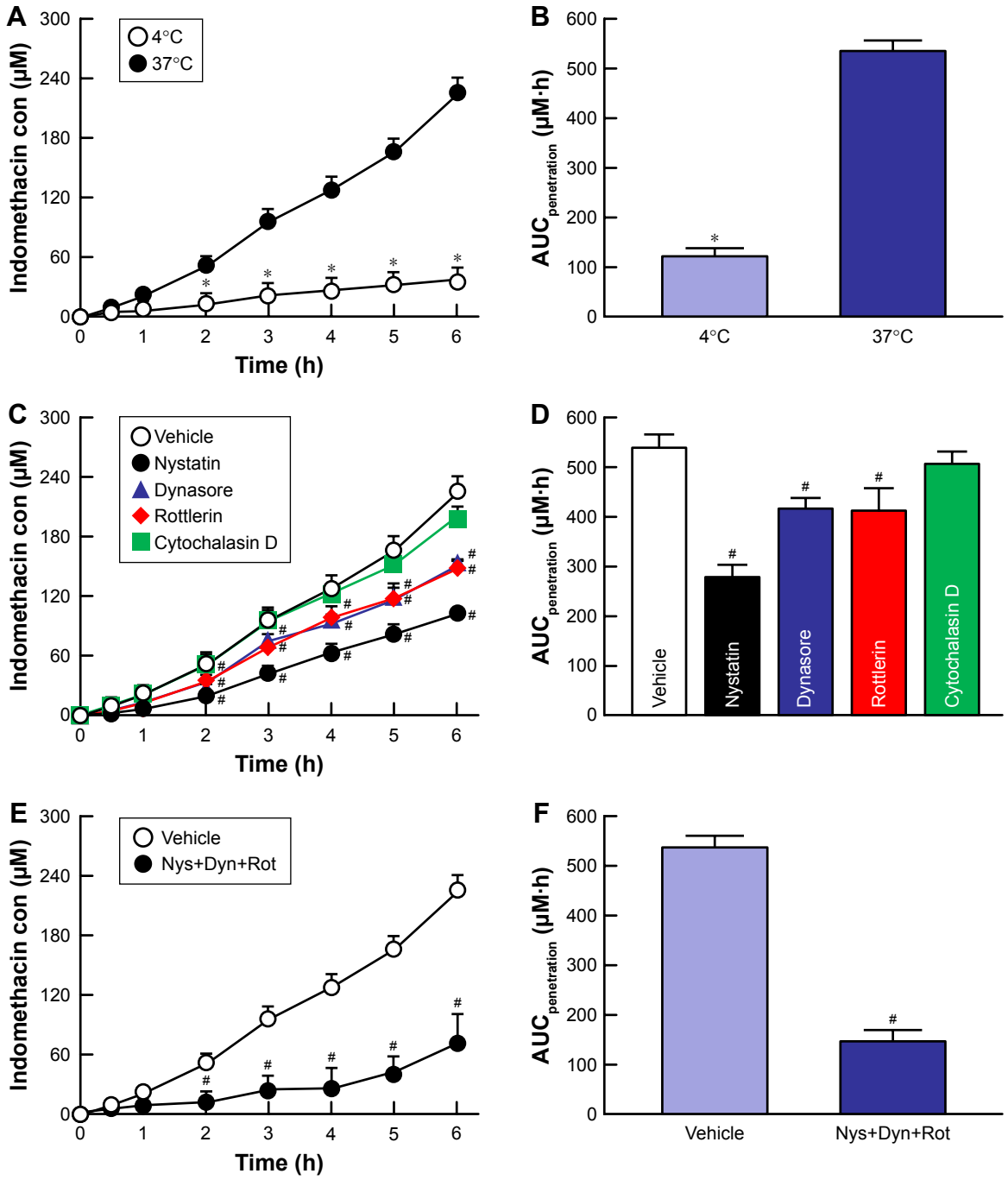

Figure 5 Effect of endocytosis pathways on in vitro transcorneal penetration of IMC-NPs in rabbit corneas.

Notes: (**A**) Penetration profile of indomethacin in IMC-NPs at 4°C and 37°C. (**B**) $AUC_{penetration}$ of indomethacin in IMC-NPs at 4°C and 37°C. Penetration profile (**C**) and $AUC_{penetration}$ (**D**) of indomethacin in IMC-NPs by treatment with individual endocytosis inhibitors. Penetration profile (**E**) and $AUC_{penetration}$ (**F**) of indomethacin in IMC-NPs by multi-treatment with nystatin, dynasore and rottlerin (Nys+Dyn+Rot). n=5–8. *$P<0.05$ vs 37°C. #$P<0.05$ vs vehicle for each category. $AUC_{penetration}$ was significantly decreased by the combination of nystatin, dynasore and rottlerin, and the decreased $AUC_{penetration}$ levels were similar to those at 4°C in rabbit cornea.

Abbreviations: $AUC_{penetration}$, area under the drug concentration–time curve in the reservoir chamber; con, concentration; IMC-NPs, ophthalmic formulation containing indomethacin nanoparticles.

ophthalmic field, is known to have a strong preservative effect, and its surface-active effects increase corneal penetration of the main component.[39] Therefore, we used 0.001% BAC in the preparation of eye drops. Mannitol (0.1%) was added to prevent the corneal stimulation caused by 0.001%–0.02% BAC.[40] It has been reported that adsorption to the surface of 5% cyclodextrin decreases the cohesion of nanoparticulate solids,[41] and 0.5% MC is essential for the preparation of drug solid nanoparticles by the bead mill method since indomethacin becomes meringue-like when subjected to the bead mill method without MC.[15] From these previous findings, we selected these additives and concentrations, and

Table 1 Pharmacokinetic analysis of the penetration of IMC-NPs in rabbit corneas treated at cold temperature (4°C) or with endocytosis inhibitors

	J_c (nmol/cm²/h)	K_p (×10⁻⁴/h)	K_m (×10⁻²)	τ (h)	D (×10⁻⁴ cm²/h)
Normal (37°C treatment)	150.6±16.2	109.8±9.7	50.8±5.3	0.51±0.03	123.2±11.8
4°C treatment	35.3±3.1*,#	28.1±2.2*,#	10.5±1.6*,#	0.92±0.10*,#	98.7±9.5*,#
Vehicle	158.4±14.7	113.3±10.7	52.4±4.8	0.48±0.04	135.2±13.1
Nystatin	88.8±8.2*,#	63.5±6.8*,#	35.0±3.9*,#	0.57±0.06	113.5±12.7
Dynasore	111.3±9.9*,#	85.3±7.3*,#	47.0±4.3	0.52±0.05	125.4±11.9
Rottlerin	111.6±9.9*,#	85.6±7.1*,#	56.8±5.3	0.54±0.07	147.7±9.1
Cytochalasin D	131.6±12.6	94.2±9.0	50.4±2.9	0.54±0.03	143.7±16.3
Nys + Dyn + Rot	40.1±4.1*,#	36.3±3.2*,#	15.9±1.5*,#	0.89±0.09*,#	99.5±9.9*,#

Notes: Parameters were calculated according to Equations 1–3 (see Materials and methods). The experiments were performed at normal (37°C) and cold (4°C) temperatures. In the study using endocytosis inhibitors, the corneal samples were co-treated with IMC-NPs and inhibitors (0.5% DMSO [vehicle], 54 μM nystatin, 40 μM dynasore, 2 μM rottlerin or 10 μM cytochalasin D). Nys + Dyn + Rot indicates the multi-treated groups, which were treated with 54 μM nystatin, 40 μM dynasore and 2 μM rottlerin. n=5–8. *$P<0.05$, vs Normal for each category. #$P<0.05$, vs Vehicle for each category.

Abbreviations: D, diffusion constant within the cornea; IMC-NPs, ophthalmic formulation containing indomethacin nanoparticles; J_c, indomethacin penetration rate; K_m, cornea/preparation partition coefficient; K_p, penetration coefficient through the cornea; τ, lag time.

designed the ophthalmic IMC-NPs used in this study. With these additives, a particle size in the nano order was obtained for the preparation of 0.5%–1% indomethacin formulations; however, the indomethacin became meringue-like for a 1.5% indomethacin formulation (high content). In order to resolve this problem, we increased the amount of MC to 2% from 0.5%. Under these conditions, ophthalmic formulations containing 1.5% indomethacin could be prepared by the bead

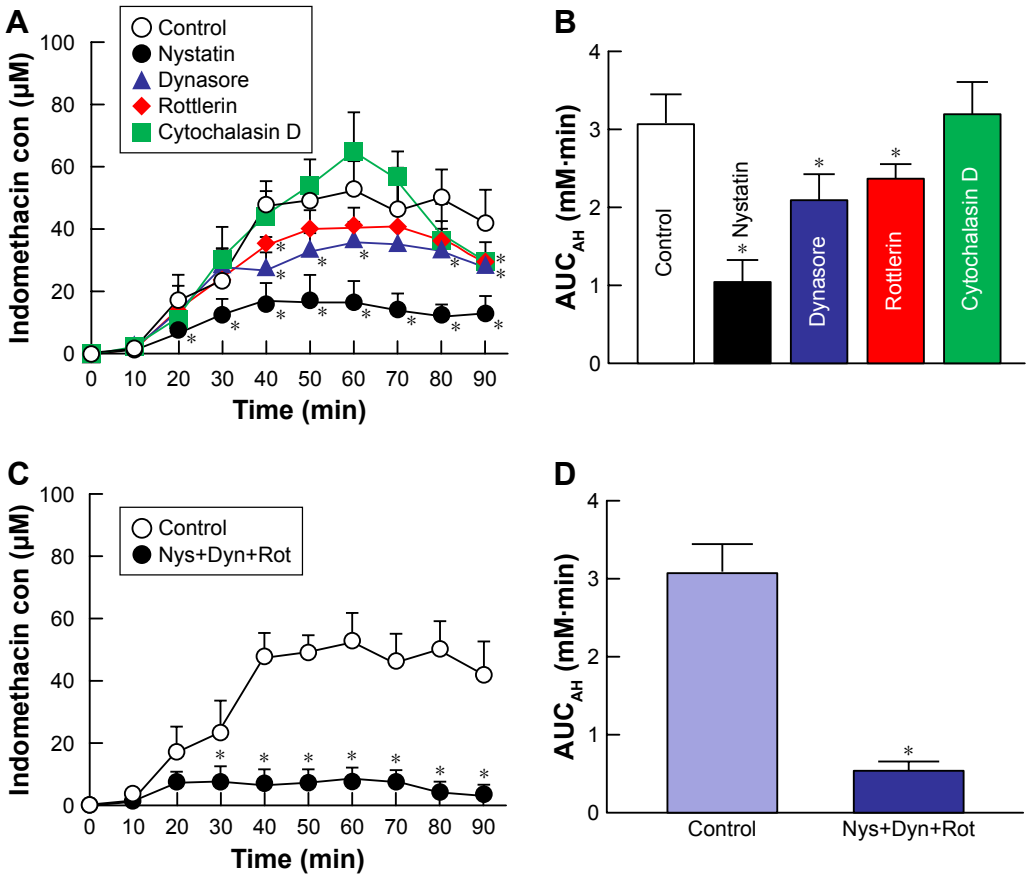

Figure 6 Effect of endocytosis pathways on in vivo transcorneal penetration of IMC-NPs in rabbit corneas.

Notes: Intraocular behavior (**A**) and AUC_{AH} (**B**) of indomethacin in IMC-NPs by treatment with individual endocytosis inhibitors. Intraocular behavior (**C**) and AUC_{AH} (**D**) of indomethacin in IMC-NPs by multi-treatment with nystatin, dynasore and rottlerin (Nys+Dyn+Rot). n=4–6. *$P<0.05$ vs control for each category. Dynasore and rottlerin tended to decrease the AUC_{AH}. On the other hand, nystatin significantly prevented transcorneal penetration. In addition, the AUC_{AH} in rabbit cornea with multi-treatment was obviously lower than that in rabbit cornea treated with each individual endocytosis inhibitor.

Abbreviations: AUC_{AH}, area under the drug concentration–time curve in the aqueous humor; con, concentration; IMC-NPs, ophthalmic formulation containing indomethacin nanoparticles.

mill treatment with a particle size of ~35–200 nm (Figure 1). The IMC-NPs in this study may be suitable to allow cellular uptake since it has been reported that nanoparticles in the size range of 60–100 nm are optimal for the cellular uptake process.[42–44] In addition, no aggregation or degradation was observed in the IMC-NPs, and the size of the indomethacin particles in IMC-NPs remained in the nano order for 14 days (Figure 2). These results show that the meringue-like consistency caused by the bead mill could be improved by increasing the MC content, and the IMC-NPs prepared with additives (BAC, mannitol, HPβCD and MC) and the bead mill method is practical for investigating the mechanism of transcorneal penetration of nanoparticles.

It is known that the corneal epithelium has a barrier function in the cornea, and we previously reported that particles <200 nm in size can penetrate the corneal tissue.[13–17] Therefore, we demonstrated the corneal epithelial penetration of indomethacin nanoparticles using HCE-T cell monolayers. Moreover, it is known that incubation at cold temperature (4°C) inhibits all energy-dependent uptake in cells including endocytosis,[31] which is the major route by which nanomedicines are transported across membranes.[24,25,37] In this study, using HCE-T cell monolayers, transepithelial penetration was prevented at 4°C (Figure 3). Although indomethacin nanoparticles were detected in the reservoir chamber under normal conditions, none were detected under cold conditions (Figure 3D). These results show that indomethacin nanoparticles can penetrate HCE-T cell monolayers, and that energy-dependent uptake contributes to this penetration. On the other hand, after penetrating the HCE-T cell monolayers, the indomethacin particles were found to be slightly aggregated (Figure 3E) with a particle size in the range of ~50–550 nm. This aggregation might be caused by the instability of the receptor medium (Hank's balanced salt solution) used in the transwell. We also investigated the transepithelial penetration pathways of indomethacin nanoparticles using endocytosis inhibitors (Figure 4). In HCE-T cell monolayers, the amount of penetration was decreased by treatment with nystatin, dynasore or rottlerin. Moreover, the amount of indomethacin penetrating the HCE-T cell monolayers treated simultaneously with nystatin, dynasore and rottlerin was similar to that observed under cold conditions. These results suggest that indomethacin nanoparticles may be taken up into HCE-T cells by three endocytosis pathways (CavME, CME and MP), and cross to the corneal stroma side.

Next, we investigated the transcorneal penetration pathways of indomethacin nanoparticles using total corneas (consisting of the corneal epithelium, stroma and endothelium) from rabbits (Figures 5 and 6). The penetration of indomethacin nanoparticles was strongly prevented at low (4°C) temperature. In addition, the $AUC_{penetration}$ and AUC_{AH} were significantly decreased by nystatin, dynasore or rottlerin (Figures 5 and 6), and the $AUC_{penetration}$ levels in corneas treated simultaneously with nystatin, dynasore and rottlerin were similar to those at 4°C (Figure 5B and F). In contrast to the results for HCE-T cell monolayers, only dissolved indomethacin (no indomethacin particles) was observed in the reservoir chamber of the transcorneal cell with total cornea under normal temperature conditions (37°C). In previous studies using intestinal epithelial cell lines (Caco-2 and HT-29), it was reported that the percent of transcytosis of nanoparticles mediated by CavME and CME was higher than that mediated by MP[45] and that the particle sizes corresponding to the CavME, CME and MP pathways are <80 nm, <120 nm and 100 nm to 5 μm, respectively.[26] Phagocytosis is performed by specialized cells such as macrophages, and plays a role in the clearance of particles with diameters >500 nm.[34,46] The particle size of indomethacin in the IMC-NPs is ~35–200 nm (mean particle size 87.8 nm). This suggests that energy-dependent endocytosis (CavME, CME and MP pathways), and, in particular, the CavME pathway, is mainly related to the penetration of indomethacin nanoparticles into the corneal epithelial membrane. Thus, the cytochalasin D (phagocytosis inhibitor) may not have prevented corneal penetration in comparison with the other inhibitors used because the particle size of the nanoparticles is smaller than 500 nm. Further, indomethacin nanoparticles that penetrate the membrane are dissolved and diffuse in the cornea, since only dissolved indomethacin was observed in the reservoir chamber (Figure 3D). From there, the dissolved indomethacin (solution type) is released into the aqueous humor (pathway 2, Figure 7). It is known that the solubility of nanoparticulates is enhanced over that of microparticulates, and the solubility of indomethacin in IMC-NPs is 4.3-fold greater than that in IMC-MPs (Figure 1E). Therefore, dissolved indomethacin in the formulation may also penetrate through the cornea and be released into the aqueous humor (pathway 1, Figure 7). In fact, indomethacin penetration was observed in the in vitro transcorneal penetration experiment using cold temperature and inhibitor treatment (Figure 5B and F). These results support previous reports indicating that nanomedicines are transported across membranes by an endocytosis pathway.[24,25,37]

Further studies are needed to elucidate the mechanism of transcorneal penetration via energy-dependent endocytosis (CavME, CME and MP pathways) of indomethacin

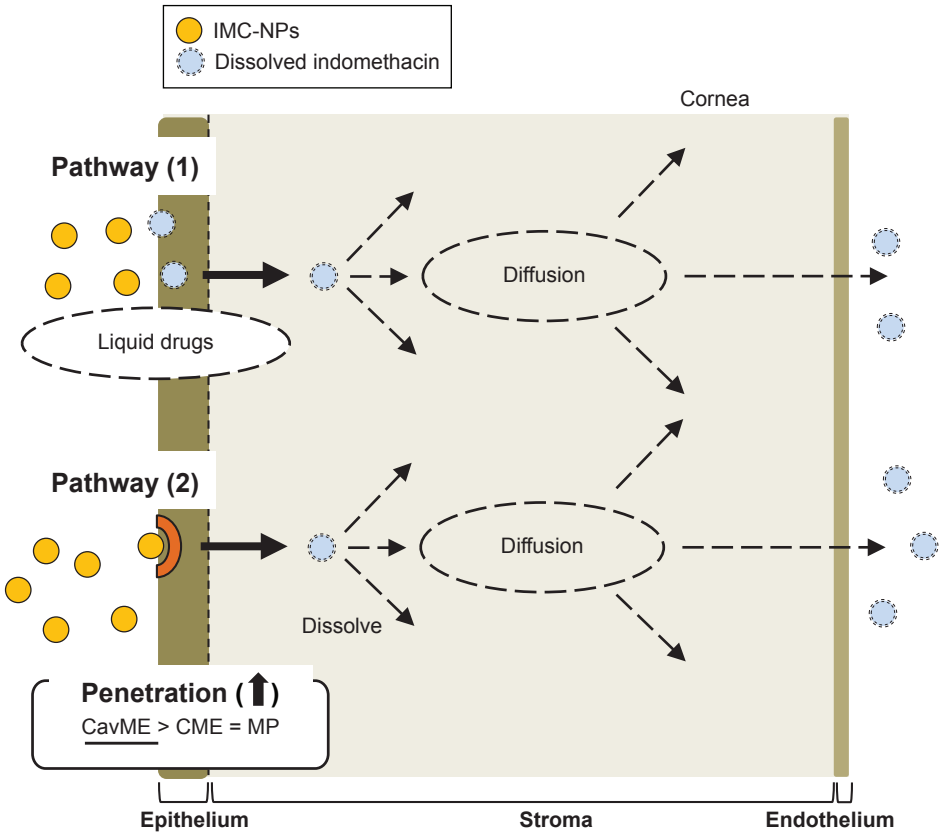

Figure 7 Mechanism for corneal penetration after the instillation of IMC-NPs.
Abbreviations: CavME, caveolae-dependent endocytosis; CME, clathrin-dependent endocytosis; IMC-NPs, ophthalmic formulation containing indomethacin nanoparticles; MP, macropinocytosis.

nanoparticles. Therefore, we are now planning to investigate the correlation between the activation of the endocytosis pathways and drug particle size using immunohistochemistry methods, and demonstrate the effect of endocytosis on indomethacin dissolution.

Conclusion

We succeeded in preparing an ophthalmic formulation containing 1.5% indomethacin nanoparticles (high content), and demonstrated that both endocytosis and transcytosis of the nanoparticles through the cornea take place. We hypothesize that indomethacin nanoparticles are taken up into the corneal epithelium by energy-dependent endocytosis (CavME, CME and MP pathways), especially CavME, and cross to the corneal stromal side. From there, the indomethacin nanoparticles are dissolved in the cornea and released into the aqueous humor in a soluble form. Our studies are the first to characterize the relationships of drug solid nanoparticles and drug delivery by energy-dependent endocytosis in the cornea, and these findings provide significant information that can be used to design further studies aimed at developing ophthalmic nanomedicines.

Author contributions

All authors contributed to data analysis, drafting and revising the article, gave final approval of the version to be published, and agree to be accountable for all aspects of the work.

Disclosure

The authors report no conflicts of interest in this work.

References

1. Toker MI, Erdem H, Erdogan H, et al. The effects of topical ketorolac and indomethacin on measles conjunctivitis: randomized controlled trial. *Am J Ophthalmol*. 2006;141(5):902–905.
2. Allegri P, Murialdo U, Peri S, et al. Randomized, double-blind, placebo-controlled clinical trial on the efficacy of 0.5% indomethacin eye drops in uveitic macular edema. *Invest Ophthalmol Vis Sci*. 2014; 55(3):1463–1470.
3. Weber M, Kodjikian L, Kruse FE, Zagorski Z, Allaire CM. Efficacy and safety of indomethacin 0.1% eye drops compared with ketorolac 0.5% eye drops in the management of ocular inflammation after cataract surgery. *Acta Ophthalmol*. 2013;91(1):e15–e21.
4. Waterbury LD, Silliman D, Jolas T. Comparison of cyclooxygenase inhibitory activity and ocular anti-inflammatory effects of ketorolac tromethamine and bromfenac sodium. *Curr Med Res Opin*. 2006;22(6):1133–1140.
5. van Haeringen NJ, van Sorge AA, Carballosa Coré-Bodelier VM. Constitutive cyclooxygenase-1 and induced cyclooxygenase-2 in isolated human iris inhibited by S(+) flurbiprofen. *J Ocul Pharmacol Ther*. 2000;16(4):353–361.

6. Diebold Y, Calonge M. Applications of nanoparticles in ophthalmology. *Prog Retin Eye Res*. 2010;29(6):596–609.
7. Chhonker YS, Prasad YD, Chandasana H, et al. Amphotericin-B entrapped lecithin/chitosan nanoparticles for prolonged ocular application. *Int J Biol Macromol*. 2015;72:1451–1458.
8. Leonardi A, Bucolo C, Drago F, Salomone S, Pignatello R. Cationic solid lipid nanoparticles enhance ocular hypotensive effect of melatonin in rabbit. *Int J Pharm*. 2015;478(1):180–186.
9. Urtti A. Challenges and obstacles of ocular pharmacokinetics and drug delivery. *Adv Drug Deliv Rev*. 2006;58(11):1131–1135.
10. Patel A, Cholkar K, Agrahari V, Mitra AK. Ocular drug delivery systems: an overview. *World J Pharmacol*. 2013;2(2):47–64.
11. Cholkar K, Patel A, Vadlapudi AD, Mitra AK. Novel Nanomicellar formulation approaches for anterior and posterior segment ocular drug delivery. *Recent Pat Nanomed*. 2012;2(2):82–95.
12. Fangueiro JF, Veiga F, Silva AM, Souto EB. Ocular Drug Delivery – New Strategies for Targeting Anterior and Posterior Segments of the Eye. *Curr Pharm Des*. 2016;22(9):1135–1146.
13. Nagai N, Nakazawa Y, Ito Y, Kanai K, Okamoto N, Shimomura Y. A nanoparticle-based ophthalmic formulation of dexamethasone enhances corneal permeability of the drug and prolongs its corneal residence time. *Biol Pharm Bull*. 2017;40(7):1055–1062.
14. Nagai N, Yoshioka C, Mano Y, et al. A nanoparticle formulation of disulfiram prolongs corneal residence time of the drug and reduces intraocular pressure. *Exp Eye Res*. 2015;132:115–123.
15. Nagai N, Ito Y, Okamoto N, Shimomura Y. A nanoparticle formulation reduces the corneal toxicity of indomethacin eye drops and enhances its corneal permeability. *Toxicology*. 2014;319:53–62.
16. Deguchi S, Otake H, Nakazawa Y, Hiramatsu N, Yamamoto N, Nagai N. Ophthalmic formulation containing nilvadipine nanoparticles prevents retinal dysfunction in rats injected with streptozotocin. *Int J Mol Sci*. 2017;18(12):2720.
17. Nagai N, Ono H, Hashino M, Ito Y, Okamoto N, Shimomura Y. Improved corneal toxicity and permeability of tranilast by the preparation of ophthalmic formulations containing its nanoparticles. *J Oleo Sci*. 2014;63(2):177–186.
18. Majumder P, Baxa U, Walsh STR, Schneider JP. Design of a multicompartment hydrogel that facilitates time-resolved delivery of combination therapy and Synergized killing of glioblastoma. *Angew Chem Int Ed*. 2018;57(46):15040–15044.
19. Zhang X, Hu W, Li J, Tao L, Wei Y. A comparative study of cellular uptake and cytotoxicity of multi-walled carbon nanotubes, graphene oxide, and nanodiamond. *Toxicol Res*. 2012;1(1):62–68.
20. Qin L, Zhang F, Lu X, et al. Polymeric micelles for enhanced lymphatic drug delivery to treat metastatic tumors. *J Control Release*. 2013;171(2):133–142.
21. Gratton SE, Ropp PA, Pohlhaus PD, et al. The effect of particle design on cellular internalization pathways. *Proc Natl Acad Sci U S A*. 2008;105(33):11613–11618.
22. Proulx ST, Luciani P, Dieterich LC, Karaman S, Leroux JC, Detmar M. Expansion of the lymphatic vasculature in cancer and inflammation: new opportunities for in vivo imaging and drug delivery. *J Control Release*. 2013;172(2):550–557.
23. Youm I, Bazzil JD, Otto JW, Caruso AN, Murowchick JB, Youan BB. Influence of surface chemistry on cytotoxicity and cellular uptake of nanocapsules in breast cancer and phagocytic cells. *Aaps J*. 2014;16(3):550–567.
24. Rappoport JZ. Focusing on clathrin-mediated endocytosis. *Biochem J*. 2008;412(3):415–423.
25. Wang J, Byrne JD, Napier ME, Desimone JM. More effective nanomedicines through particle design. *Small*. 2011;7(14):1919–1931.
26. Zhang S, Li J, Lykotrafitis G, Bao G, Suresh S. Size-dependent endocytosis of nanoparticles. *Adv Mater*. 2009;21(4):419–424.
27. Vercauteren D, Vandenbroucke RE, Jones AT, et al. The use of inhibitors to study endocytic pathways of gene carriers: optimization and pitfalls. *Mol Ther*. 2010;18(3):561–569.
28. Dausend J, Musyanovych A, Dass M, et al. Uptake mechanism of oppositely charged fluorescent nanoparticles in HeLa cells. *Macromol Biosci*. 2008;8(12):1135–1143.
29. Raghu H, Sharma-Walia N, Veettil MV, Sadagopan S, Chandran B. Kaposi's sarcoma-associated herpesvirus utilizes an actin polymerization-dependent macropinocytic pathway to enter human dermal microvascular endothelial and human umbilical vein endothelial cells. *J Virol*. 2009;83(10):4895–4911.
30. Qualmann B, Kessels MM, Kelly RB. Molecular links between endocytosis and the actin cytoskeleton. *J Cell Biol*. 2000;150(5):F111–F116Review.
31. He Z, Liu K, Manaloto E, et al. Cold atmospheric plasma induces ATP-dependent endocytosis of nanoparticles and synergistic U373MG cancer cell death. *Sci Rep*. 2018;8(1):5298.
32. Araki-Sasaki K, Ohashi Y, Sasabe T, et al. An SV40-immortalized human corneal epithelial cell line and its characterization. *Invest Ophthalmol Vis Sci*. 1995;36(3):614–621.
33. Nagai N, Inomata M, Ito Y. Contribution of aldehyde dehydrogenase 3A1 to disulfiram penetration through monolayers consisting of cultured human corneal epithelial cells. *Biol Pharm Bull*. 2008;31(7):1444–1448.
34. Mäger I, Langel K, Lehto T, Eiríksdóttir E, Langel U. The role of endocytosis on the uptake kinetics of luciferin-conjugated cell-penetrating peptides. *Biochim Biophys Acta*. 1818;2012:502–511.
35. Malomouzh AI, Mukhitov AR, Proskurina SE, Vyskocil F, Nikolsky EE. The effect of dynasore, a blocker of dynamin-dependent endocytosis, on spontaneous quantal and non-quantal release of acetylcholine in murine neuromuscular junctions. *Dokl Biol Sci*. 2014;459(1):330–333.
36. Hufnagel H, Hakim P, Lima A, Hollfelder F. Fluid phase endocytosis contributes to transfection of DNA by PEI-25. *Mol Ther*. 2009;17(8):1411–1417.
37. Longfa K, Jin S, Yinglei Z, Zhonggui H. The endocytosis and intracellular fate of nanomedicines: implication for rational design. *Asian J Pharm Sci*. 2013;8:1–10.
38. Calvo P, Alonso MJ, Vila-Jato JL, Robinson JR. Improved ocular bioavailability of indomethacin by novel ocular drug carriers. *J Pharm Pharmacol*. 1996;48(11):1147–1152.
39. Pisella PJ, Fillacier K, Elena PP, Debbasch C, Baudouin C. Comparison of the effects of preserved and unpreserved formulations of timolol on the ocular surface of albino rabbits. *Ophthalmic Res*. 2000;32(1):3–8.
40. Nagai N, Murao T, Oe K, Ito Y, Okamoto N, Shimomura Y. An in vitro evaluation for corneal damages by anti-glaucoma combination eye drops using human corneal epithelial cell (HCE-T). *Yakugaku Zasshi*. 2011;131(6):985–991.
41. Mori K, Yoshioka N, Kondo Y, Takeuchi T, Yamashita H. Catalytically active, magnetically separable, and water-soluble FePt nanoparticles modified with cyclodextrin for aqueous hydrogenation reactions. *Green Chem*. 2009;11(9):1337–1342.
42. Gao H, Shi W, Freund LB. Mechanics of receptor-mediated endocytosis. *Proc Natl Acad Sci U S A*. 2005;102(27):9469–9474.
43. Zhang S, Gao H, Bao G. Physical principles of nanoparticle cellular endocytosis. *ACS Nano*. 2015;9(9):8655–8671.
44. Chithrani BD, Chan WC. Elucidating the mechanism of cellular uptake and removal of protein-coated gold nanoparticles of different sizes and shapes. *Nano Lett*. 2007;7(6):1542–1550.
45. Yang D, Liu D, Qin M, et al. Intestinal mucin induces more endocytosis but less transcytosis of nanoparticles across enterocytes by triggering nanoclustering and strengthening the retrograde pathway. *ACS Appl Mater Interfaces*. 2018;10(14):11443–11456.
46. Aderem A, Underhill DM. Mechanisms of phagocytosis in macrophages. *Annu Rev Immunol*. 1999;17(1):593–623.